ACS OMEGA

Article

Cite This: ACS Omega 2019, 4, 7543−7549

http://pubs.acs.org/journal/acsodf

Simultaneous Removal of Multiple Heavy Metal Ions from River Water Using Ultrafine Mesoporous Magnetite Nanoparticles

Tano Patrice Fato,[†] Da-Wei Li,[†] Li-Jun Zhao,[†] Kaipei Qiu,*[,†] and Yi-Tao Long[†,‡]

[†]School of Chemistry and Molecular Engineering, East China University of Science and Technology, 130 Meilong Road, Shanghai 200237, China

[‡]State Key Laboratory of Analytical Chemistry for Life Science, School of Chemistry and Chemical Engineering, Nanjing University, 163 Xianlin Avenue, Nanjing 210039, China

Supporting Information

ABSTRACT: The exploration of simultaneous removal of co-existing or multiple pollutants from water by the means of nanomaterials paves a new avenue that is free from secondary pollution and inexpensive. In the aquatic environment, river water contains a mixture of ions, which can influence the adsorption process. In this respect, removing heavy metal ions becomes a true challenge. Here, four heavy metal ions, namely, Pb^{2+}, Cd^{2+}, Cu^{2+}, and Ni^{2+}, have been successfully removed simultaneously from river water using ultrafine mesoporous magnetite (Fe_3O_4) nanoparticles (UFMNPs) based on the affinity of these metal ions toward the UFMNP surfaces as well as their unique mesoporous structure, promoting the easy adsorption. The individual removal efficiencies of Pb^{2+}, Cd^{2+}, Cu^{2+}, and Ni^{2+} ions from river water were 98, 87, 90, and 78%, respectively, whereas the removal efficiencies of the mixed Pb^{2+}, Cd^{2+}, Cu^{2+}, and Ni^{2+} ions were 86, 80, 84, and 54%, respectively, in the same river water. Thus, the data clearly indicate the complex removal of heavy metal ions in multi-ion systems. This study has demonstrated the huge potential of UFMNPs to be effective for their use in wastewater treatment, especially to simultaneously remove multiple heavy metal ions from aqueous media.

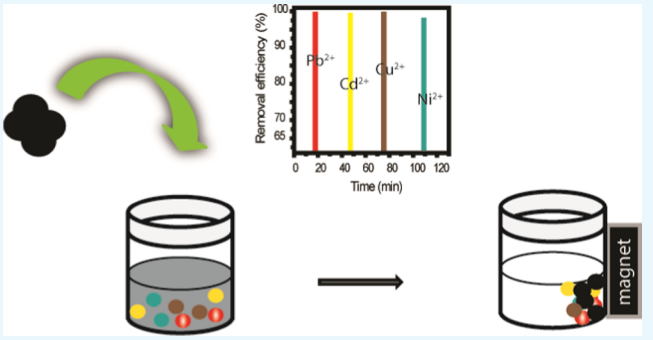

INTRODUCTION

Heavy metal ions (HMIs) are ubiquitous pollutants in the environment, and in particular, the existence of HMIs such as Pb^{2+}, Cd^{2+}, Cu^{2+}, and Ni^{2+} in river water is of great concern because of their severe threats to public health, living organisms, and freshwater supply.[1,2] For instance, the exposure to the excessive levels of such HMIs significantly increases the likelihood of kidney damage, nervous system damage, and renal dysfunction as they are nonbiodegradable.[3,4] To eliminate these potential harmful health effects, environmental regulations to reduce the HMIs concentration in water are becoming increasingly stringent.[5] Simultaneous removal of a mixture of several hazardous HMIs offers a cost-effective solution. It has been, however, quite challenging to date due to the competing adsorption of these HMIs. Meanwhile, it is highly requested so as to avoid the repeated one-by-one removal of pollutants and of course to develop an attractive low-cost strategy.

To achieve the removal of HMIs from different effluents, conventional methods including chemical precipitation, membrane filtration, and adsorption have been developed.[6] Of all of the various treatment technologies, adsorption is one of the techniques generally used due to its cost-effectiveness and flexibility in design and operation.[3,7,8] In this way, numerous adsorbents have been developed and used for the removal of pollutants from water/wastewater including activated carbon, zeolite, polymeric materials, fly ash, and biomass.[7,9] Although they may be effective for HMI removal, they have many disadvantages including complexity, high cost, and secondary waste and have low adsorption capacities, which limit their use in water/wastewater treatment. Hence, there is a need to design and explore new adsorbents with improvements in adsorption capacity, superior separation rate, and ease of operation.

Magnetic nanoparticles (NPs) with particle sizes less than 40 nm are easily dispersible in solutions, exhibiting a large surface area and superparamagnetic properties, and can be attracted by an externally applied magnetic field but do not retain magnetic properties when the field is removed.[10] This magnetic property makes them effective adsorbents for HMI removal and highly useful in novel separation processes. In particular, more recently, magnetite (Fe_3O_4) NPs have been found to be great adsorbents for water purification as they are recognized to exhibit high ratio of area to volume and fast

Received: March 15, 2019
Accepted: April 16, 2019
Published: April 24, 2019

DOI: 10.1021/acsomega.9b00731
ACS Omega 2019, 4, 7543−7549

magnetic response and adsorption kinetics.[11] Additionally, magnetite nanoparticles are nontoxic, recyclable, and easy to synthesize, and co-precipitation method is a simple and efficient way to produce them.[2] For these reasons, monodisperse magnetite NPs were used to remove arsenic from water with magnetic capture at an extremely low magnetic field gradient.[12] The reduction of the size of Fe_3O_4 NPs from 300 to 12 nm also increased by orders of magnitude the removal efficiency of As(V) and orange II from solution.[12] Besides, magnetite NPs with small sizes have been synthesized and used for removal of heavy metal ions such as Tc(VII) and Cr(VI),[13] As(III),[6] Hg(II),[14] and As(V)[15] from aqueous solutions. These studies have been carried out to date on the single adsorption of heavy metal ions onto bare Fe_3O_4 NPs.[3,7,16] As such, the aim of this study is to investigate the single and multicomponent adsorption of Pb^{2+}, Cd^{2+}, Cu^{2+}, and Ni^{2+} ions from natural water using pristine Fe_3O_4 NPs since information about simultaneous adsorption of HMIs in multicomponent systems on bare Fe_3O_4 NPs is scare so far and should be explored. The natural water was used because it contains multiple types of these metal ions and its environment is complicated.

Herein, ultrafine magnetite NPs were synthesized by co-precipitation method and successfully used as adsorbents for the removal of four mixed metal ions (Pb^{2+}, Cd^{2+}, Cu^{2+}, and Ni^{2+}) from contaminated river water, which represents hitherto the greatest application in removal of metal ions by magnetite NPs. The key to this success was based on the mesoporous property exhibited by the magnetite NPs, which, to the best of our knowledge, has not never explored to date. Indeed, river water was used because groundwater and surface water contain a complex mixture of ions and organic matters, which mimics well a concrete practical application. The important factors including medium pH, temperature, contact time, adsorbent amount, and initial metal ion concentration as well as thermodynamic parameters were investigated. Also, the easy regeneration of the magnetite nanoadsorbents was carried out using diluted nitric acid at pH 1.

RESULTS AND DISCUSSION

Characterization of the Ultrafine Magnetite Nanoparticles. The powder X-ray diffraction (XRD) pattern of Fe_3O_4 is shown in Figure 1a. All of the diffraction peaks with 2θ at 30.15, 35.37, 43.31, 53.69, 57.08, 62.77, 71.48, and 74.34° are attributed to crystal planes of Fe_3O_4(220), (311), (400), (422), (511), (440), (620), and (533), respectively. Therefore, the XRD results confirm the successful synthesis of Fe_3O_4 NPs and show good consistency with the standard pattern of Fe_3O_4 (PDF card 19-0629). Moreover, no other significant peaks were observed. This observation indicates that the synthesized Fe_3O_4 NPs do not contain any other crystallite impurities. The calculated average crystallite size was 9 nm, which indicates that ultrafine Fe_3O_4 NPs were formed[17] using Debye Scherrer equation based on the line-broadening of the magnetite (311) reflection and expressed by[16]

$$D = \frac{p\lambda}{\delta \cos \alpha} \quad (1)$$

where δ is the full width at half-maximum (FWHM) in radian, α is Bragg's angle, λ is the wavelength of the incident X-rays, p is a constant (0.9), and D is the diameter.

Details about the structure and morphology of the Fe_3O_4 NPs were examined with TEM (Figure 1b). Through visual observation, we found that the small spherical particles tend to aggregate due to the magnetic forces between them. This tendency of ultrafine mesoporous magnetite (Fe_3O_4) nanoparticles (UFMNPs) to aggregate was attributed to the absence of stabilizing surfactants deliberately omitted during their synthesis to ensure that UFMNPs surface sites remain exposed and active for better characterizing the adsorption of the different studied metal ions. The average size of the particles is estimated to vary between 4 and 17 nm. Thus, the smaller magnetite NPs exhibited a high dispersion capability in water.[16,18,19]

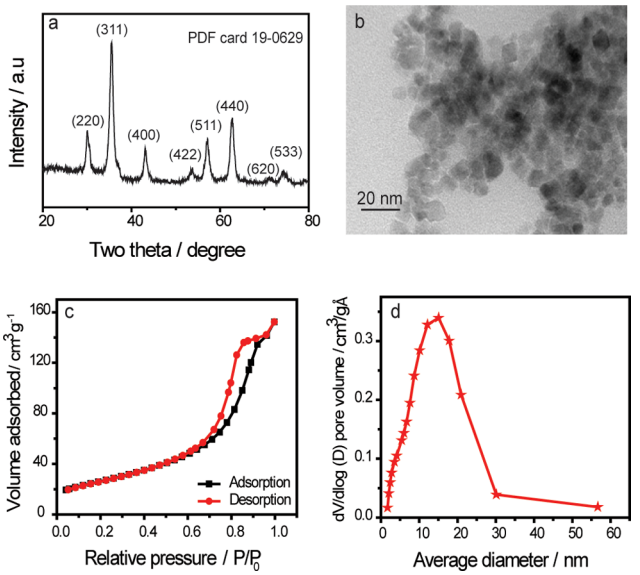

Figure 1. Characterizations of the prepared magnetite nanoparticles. (a) Powder X-ray diffraction (XRD) pattern, (b) transmission electron microscopy (TEM) image, (c) N_2 adsorption−desorption isotherms, and (d) average pore size of Fe_3O_4 nanoparticles.

Figure 1c shows the Brunauer−Emmett−Teller (BET) analysis of the prepared Fe_3O_4 NPs, which revealed a relative high surface area of 94.43 $m^2\ g^{-1}$. Physical properties such as surface area, pore volume, and average pore diameter of Fe_3O_4 NPs are listed in Table 1. Besides, the nitrogen adsorption/desorption isotherm of UFMNPs was similar to the type IV isotherms, proving indeed the presence of mesopores according to the BET classification unlike previously reported nonporous structures of magnetite.[20,21] This mesoporous structure displayed thus effective transport pathways to the interior cavities, which could further increase the adsorption capacity of UFMNPs.[22] The formation of the mesoporous Fe_3O_4 NPs structure is due to the addition of hydrazine during thermal treatment at 85 °C.[23,24] The particles have a spherical form, so the specific surface area can enable the determination of the average particle diameter by the following equation[25]

Table 1. Physical Properties of Fe_3O_4 Nanoparticles

sample	surface area ($m^2\ g^{-1}$)	average pore diameter (nm)	pore size (nm)	pore volume ($cm^3\ g^{-1}\ Å^{-1}$)
Fe_3O_4	94.43	15	2−60	0.02−0.35

$$D_{BET} = 600/\partial S \quad (2)$$

where ∂ is the theoretical density in g cm^{-3}, S is the specific surface area in $m^2\ g^{-1}$, and D_{BET} is the average particle diameter in nm.

DOI: 10.1021/acsomega.9b00731
ACS Omega 2019, 4, 7543−7549

Consequently, the average particle size of 17.41 nm was evaluated, consistent with the TEM results. Figure 1d indicates the pore size in the range of 2−60 nm, and the average diameter was around 15 nm shown by the strong peak.

Performances of Ultrafine Magnetite Nanoparticles in Deionized Water and Natural Water. Figure 2 depicts the application of UFMNPs in contaminated deionized water and natural water for the removal of Pb^{2+}, Cd^{2+}, Cu^{2+}, and Ni^{2+} ions at ambient temperature. In this regard, the removal of these metal ions from deionized water shows a rapid adsorption of Pb^{2+}, Cd^{2+}, and Cu^{2+} where more than 90% was adsorbed within 20 and 40 min for Ni^{2+}. Over this period, the rate of the metal ion uptake slowly decreased and gradually did not seem to increase any further (Figure 2a). These observations can be explained by the fact that at the beginning of the adsorption process there was more availability of active sites on the Fe_3O_4 NP adsorbents, and with the accumulation time, these sites slowly saturated.[26] Thus, the removal efficiencies of Pb^{2+}, Cd^{2+}, Cu^{2+}, and Ni^{2+} ions were 99.6, 99.1, 99.2, and 98.3%, respectively. The same trend was observed with the individual removal of the studied HMIs in the river water (Figure 2b) but with longer removal time and less removal efficiency during both steps described above. Actually, the first step lasted 100 min for Pb^{2+}, Cd^{2+}, and Cu^{2+} where 97.60, 86.60, and 89.51% were adsorbed, respectively. For Ni^{2+} ions, it needed 120 min and its removal efficiency was 77.50%. Then, the uptake slowed down for all of the metal ions and did not increase any further over time. The uptake of these metal ions was retarded and decreased in the river water by the presence of other substances including ions and organic matters, which likely blurred the adsorption of the metal ions and filled up the pores on the Fe_3O_4 NP adsorbents.

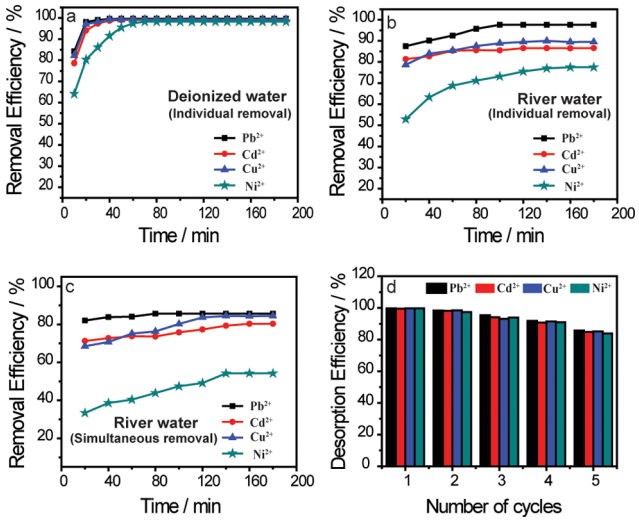

Figure 2. Application of ultrafine magnetite nanoparticles in different types of water. Individual removal of Pb^{2+}, Cu^{2+}, Cd^{2+}, and Ni^{2+} ions from contaminated (a) deionized water and (b) river water. (c) Simultaneous removal of Pb^{2+}, Cu^{2+}, Cd^{2+}, and Ni^{2+} ions from river water. (d) Number of succeeding cycles using diluted nitric acid at pH 1.0. (For 50 mL of deionized water, initial concentration of 10 mg L^{-1}, 50 mg of Fe_3O_4 NPs, initial pH of solution 5.5 were used, and for 50 mL of river water, initial concentration of 50 mg L^{-1}, 100 mg of Fe_3O_4 NPs, initial pH of solution 6.5, and temperature of 25 °C were used).

To further demonstrate the performance of the UFMNPs, the simultaneous removal of these HMIs was carried out in the river water (Figure 2c). Upon comparing the removal efficiency of the previous individual removals, it was clear that the uptake of the studied HMIs was further decreased in simultaneous removal, even though both steps were also observed. This was assigned to the competitive adsorption of these HMIs at a time that hindered the uptake process, indicating that the adsorption of the metal ions depended on each other. In addition, the reduced equilibrium capacity values of metal ions adsorbed onto Fe_3O_4 adsorbents clearly demonstrated the competition between heavy metal ions for the available surface area. Preferential adsorption of heavy metal ions from the mixture was inherent to the affinity of these HMIs toward Fe_3O_4 adsorbents, as determined from single removal analysis (Table S1). After 180 min, the removal efficiencies of Pb^{2+}, Cd^{2+}, Cu^{2+}, and Ni^{2+} ions were 85.62, 80.31, 84.41, and 54.20%, respectively. These results showed additional reasons to the foregoing findings during the

Scheme 1. Removal of Heavy Metal Ions from Aqueous Medium Following the Desorption Process[a]

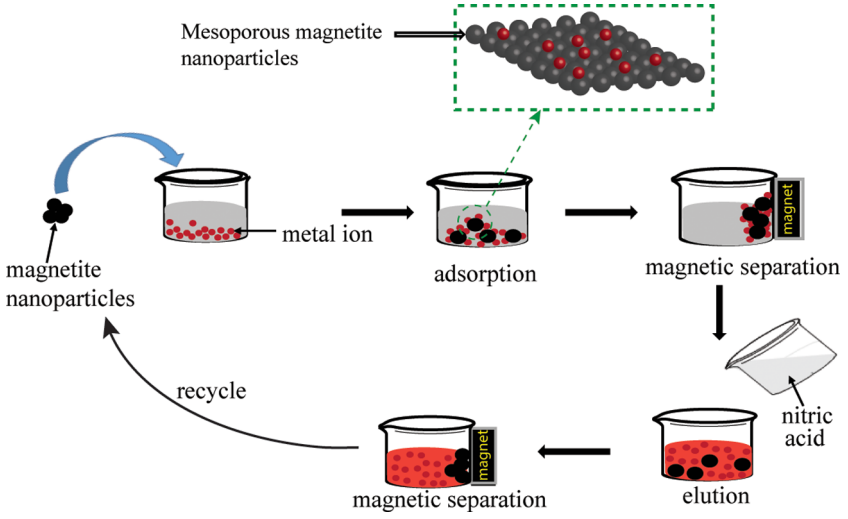

[a]The dashed rectangle shows the adsorption of metal ions across mesoporous magnetite nanoparticles.

DOI: 10.1021/acsomega.9b00731
ACS Omega 2019, 4, 7543−7549

simultaneous uptake, namely, the electropositivity of the ions,[27] hydrated ionic radii,[18] ionic strength of the solution,[28] concentration of the metal ions,[29] and precipitation and surface complexation.[30] Nevertheless, it is noteworthy that the simultaneous removal of four ions has been achieved even if the removal efficiency was less than 90% for each ion, and one could attribute the key to this success of simultaneous removal of these metal ions to the large ratio of the surface area to volume, mesoporous property, and relative huge pore volume (0.02−0.35 $cm^3\ g^{-1}\ Å^{-1}$) of the UFMNPs. Also, we extended the previous results by the aggregation observed in the TEM image, which promoted the easy adsorption of the ions via the overlapping of the adsorption sites of the naked Fe_3O_4 NP adsorbents.

In the adsorption process, the desorption and repeatability are significant parameters for developing new adsorbents for practical applications. The desorption study was carried out to examine the recyclability and regeneration of the adsorbents in synthetic water. To do so, the studied heavy metal ions (i.e., Pb^{2+}, Cd^{2+}, Cu^{2+}, and Ni^{2+}) adsorbed by UFMNPs were released (Scheme 1) using diluted nitric acid (0.01 M) at different pH values such as pH 1.0, pH 2.0, and pH 3.0, and the results are shown in Figure S4. As can be observed, the pH 1.0 was more suitable to restore the used adsorbents since the desorption efficiency decreases with the increasing pH. The reusability of the UFMNPs was thus tested by successively applying the adsorption/desorption cycle using the same adsorbents in deionized water using diluted nitric acid (0.01 M) at pH 1.0. Figure 2d illustrates the removal efficiency of the studied metal ions in several cycles (five cycles) using Fe_3O_4 NPs. It is found that the Fe_3O_4 nanoadsorbents can retain nearly 85% of their initial adsorption capacity after five succeeding adsorption/desorption cycles, which confirms their effective recoverability in diluted nitric acid at pH 1.0.

Tests of the Metal Ion Adsorption. To characterize the dependence of metal ion adsorption on different parameters and their nature, we performed the adsorption process in synthetic water (for more parameters, see the Supporting Information, SI).

Effect of pH on Metal Ion Adsorption. In the adsorption process, the pH of the medium remains a fundamental controlling parameter that affects the metal chemistry in solution and the actives sites of the adsorbent.[30] To this aim, the influence of pH on the removal efficiency of heavy metal ions by UFMNPs was assessed over a wide pH range from 2 to 12 and is shown in Figure 3a. As can be seen in this figure, the increase in the pH leads to the increase in the removal efficiency for all tested metal ions until pH = 6, beyond which the removal efficiency remains almost constant. One reason may be the fact that at lower pH the proton (H^+) density in the medium is higher, and then, a competition between H^+ and metal ions can occur at the active sites of the Fe_3O_4 nanoadsorbents rendering the active adsorption sites less available for metal ions.[31] As the adsorption mechanism is a surface process, the surface of the adsorbent is of great importance for the extent of adsorption and is a key quality parameter. Therefore, the other reason was ascribed to the surface charge of the Fe_3O_4 nanoadsorbents since magnetite NPs exhibit amphoteric surface activity.[18]

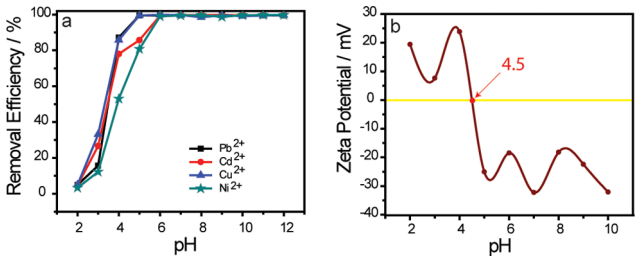

Figure 3. (a) Effect of pH on the removal of Cu^{2+}, Cd^{2+}, Ni^{2+}, and Pb^{2+} ions by Fe_3O_4 nanoparticles at 25 °C (the initial concentration of 10 mg L^{-1}, pH 5.5). (b) Effect of solution pH on the ζ-potential of Fe_3O_4 nanoparticles.

In aqueous media, the surface of magnetite NPs is recovered by FeOH. As such, it can be deprotonated or protonated to lead to FeO^- or $Fe(OH)_2^+$ according to the pH of the medium. Furthermore, to understand the adsorption of charged species and the impact of pH, the ζ-potential of the UFMNPs was recorded at different pH values and is depicted in Figure 3b. As can be seen in this figure, the potential of zero charge (PZC) of the UFMNPs is 4.5, consistent with the literature,[7] where their total charge is considered zero as the positive charges and negative charges are equal. Below pH_{PZC} (4.5), the positive charges are predominant onto the Fe_3O_4 NP adsorbents; therefore, an electrostatic repulsion existed between heavy metal ions and their surfaces, which illustrates the weak removal efficiency of the different metal ions at low pH. In contrast, the surface of the UFMNPs becomes negatively charged (FeO^-) beyond pH_{PZC} (4.5), promoting metal ions' electrostatic attraction. This explains the increase in the uptake of the different metal ions at higher pH values. Nevertheless, at some point (pH > 6) it was found that the removal efficiency decreases with the increasing pH of the solution because different metal ions began precipitating.[7,32] Moreover, at 25 °C, the solubility product constants of $Pb(OH)_2$, $Cd(OH)_2$, $Cu(OH)_2$, and $Ni(OH)_2$ are 1.43×10^{-20}, 7.20×10^{-15}, 2.00×10^{-15}, and 5.48×10^{-16}, respectively. It has been found that the removal of heavy metal ions may occur owing to the formation of hydroxide precipitation at pH values higher than 6.[7,16,33] Hence, the removal of heavy metals at high pH (pH > 6) introduced uncertainty with respect to adsorption against precipitation.[3,34] For this reason, the solution of pH 5.5 was selected throughout the removal experiments.

To test the stability of the prepared Fe_3O_4 NPs, the leaching of iron ions was investigated during the adsorption of the different metal ions at different pH values in synthetic water. Table 2 summarizes this leaching after suspending 50 mg of Fe_3O_4 NPs in 50 mL of metal ion solution for 2 h. The results indicated that the leaching of iron ions was negligible with respect to the total iron even though the values in more acidic solution (pH 2.0) were the highest ones for all of the tested

Table 2. Leaching of Fe after Suspending 50 mg of Fe_3O_4 NPs in 50 mL of Different Metal Ion Solutions for 2 h

	percentage of Fe leached per total Fe during metal ion adsorption			
pH	Pb^{2+}	Cd^{2+}	Cu^{2+}	Ni^{2+}
2	0.07	0.066	0.056	0.099
4	0.0016	0.0037	0.0020	0.0046
6	0.0022	0.0056	0.0022	0.0045
8	0.0059	0.0030	0.0044	0.0060
10	0.0062	0.0070	0.0019	0.0029
12	0.0087	0.0021	0.0026	0.0095

DOI: 10.1021/acsomega.9b00731
ACS Omega 2019, 4, 7543−7549

metal ions. Consequently, the pH of the medium did not affect the adsorbents (Fe_3O_4 NPs).

Adsorption Kinetics. The adsorption kinetics is one of the important characteristics defining the effectiveness of an adsorbent, which describes the solute uptake rate by controlling the diffusion process and the residence time of an adsorbate uptake at the solid/solution interface. To evaluate the nature of the adsorption mechanism and the efficiency of the UFMNPs, two widely used kinetic models such as the pseudo-first-order and pseudo-second-order kinetic models were investigated to analyze the experimental results (for brevity, the relative equations are given in SI). Figure 4 depicts

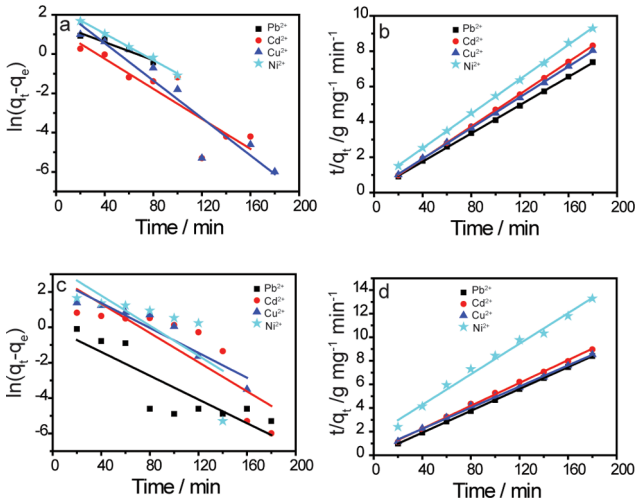

Figure 4. Fitting of different kinetic models for Cu^{2+}, Cd^{2+}, Ni^{2+}, Pb^{2+} ion adsorption onto Fe_3O_4 NPs. (a) Physical adsorption (physisorption) and (b) chemical adsorption (chemisorption) models for single adsorption. (c) Physical adsorption (physisorption) and (d) chemical adsorption (chemisorption) models for competitive adsorption.

the linear plot of the mentioned adsorption kinetic models of the separate and simultaneous process of these heavy metal ions. The results of the calculated kinetic parameters are listed in Table S2. From this table, the pseudo-second-order model with its higher correlation coefficient (R^2) for all tested metal ions described the adsorption process better than the pseudo-first-order model using Fe_3O_4 NPs, showing quite a good linearity (Figure 4b,d). This observation denotes that the adsorption process was controlled by chemisorption.[35] Moreover, the values of calculated equilibrium capacities q_e (cal.) resulting from the pseudo-second-order model were more consistent with experimental q values q_e (exp.) than those calculated from the pseudo-first-order model. However, decreased values of the quantity of heavy metal ions adsorbed onto Fe_3O_4 NPs from mixed metal ion solutions compared to the single ion solution ones markedly illustrated the competition between the different heavy metal ions for the accessible active sites on the adsorbents. The results in this quaternary Pb−Cd−Cu−Ni system indicated that the rate constant of Pb^{2+} (0.045 g mg^{-1} min^{-1}) was higher than the rate constants of Cu^{2+} (0.008 g mg^{-1} min^{-1}), Cd^{2+} (0.005 g mg^{-1} min^{-1}), and Ni^{2+} (0.003 g mg^{-1} min^{-1}), further demonstrating the strong affinity of Fe_3O_4 NPs for Pb^{2+}. Additionally, it significantly showed the inhibition effect of Pb^{2+} in the competitive adsorption of multicomponent systems.[30]

Effect of Initial Metal Ion Concentration and Adsorption Isotherms. The initial concentration remains a fundamental parameter that allows ascertaining the adsorption capacity of an adsorbent. Figure S7 represents the experimental results of the influence of initial metal ion (Pb^{2+}, Cd^{2+}, Cu^{2+}, Ni^{2+}) concentrations on the removal efficiency obtained in the range of 10−150 mg L^{-1}. It is clear that with an increase in metal ion concentrations the uptake efficiency of all studied metal ions gradually decreased. This observation can be explained by the fact that at low metal ion concentration the ratio number of moles of metal ions to the active sites of the Fe_3O_4 nanoadsorbents is large and thereby the fractional adsorption becomes independent of initial metal ion concentration.[4] However, when the metal ion concentration increases, the available active sites on the Fe_3O_4 nanoadsorbents become fewer compared with the available number of moles of metal ions, leading to the decrease in the adsorption efficiency of metal ions.[36]

To determine the nature of the interaction between all tested metal ions and the Fe_3O_4 nanoadsorbents, and find the maximum capacity of these nanoadsorbents, the adsorption data were examined using adsorption isothermal models such as Langmuir, Freundlich, Dubinin−Radushkevich, and Temkin isotherm models. (See the Supporting Information regarding the assumptions and equations related to each model.) Figure 5 shows the different isotherm models used for characterizing

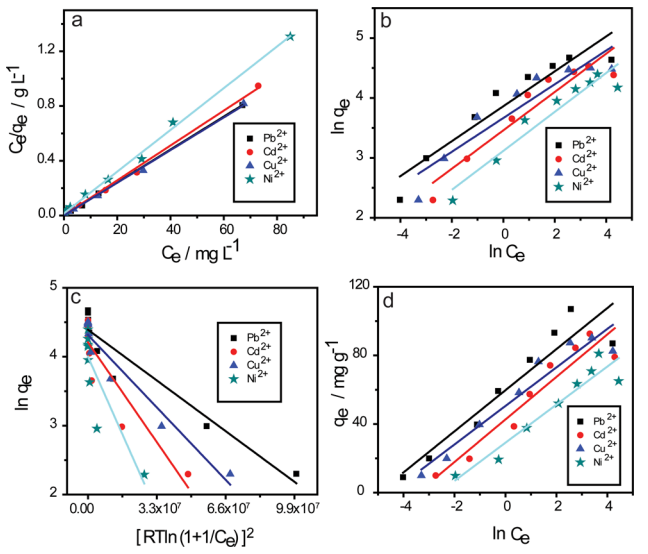

Figure 5. Equilibrium isotherm models for examining the adsorption process. (a) Langmuir, (b) Freundlich, (c) Dubinin−Radushkevich, and (d) Temkin isotherm models adsorption for Pb^{2+}, Cd^{2+}, Cu^{2+}, and Ni^{2+} ions onto Fe_3O_4 NPs.

the adsorption of Pb^{2+}, Cd^{2+}, Cu^{2+}, and Ni^{2+} onto the UFMNPs, and the entire calculated isotherm parameters from these models are listed in Table S3. From these results, the adsorption of the tested ions is well described by the Langmuir isotherm model where the correlation coefficient is closer to unity. This demonstrates that the active sites onto the Fe_3O_4 NPs disperse homogeneously and the adsorbed metal ions cover the NPs surface by forming a monolayer. Besides, the adsorption can occur only at a fixed number of definite identical and equivalent localized sites. The adsorption of the tested metal ions was based on the electrostatic attraction between them and the Fe_3O_4 NP surfaces. According to the

DOI: 10.1021/acsomega.9b00731
ACS Omega 2019, 4, 7543−7549

Langmuir model results, the maximum adsorption capacities of Pb^{2+}, Cd^{2+}, Cu^{2+}, and Ni^{2+} onto the UFMNPs were 85, 79, 83, and 66 mg g^{-1}, respectively. Also, the R_L values of the Langmuir model for all studied metal ions lied in the range of 0−1, illustrating favorable adsorption of these metal ions by Fe_3O_4 NP adsorbents. The adsorption intensity n from the Freundlich model of the tested metal ions was in the range of 1−10, indicating also a favorable adsorption process.[37] Based on the Dubinin−Radushkevich model, the values of ε (kJ mol^{-1}) for all studied metal ions were higher than 8, confirming that the attractive forces were chemical bonding (chemisorption).[38] The relatively high values of the Temkin isotherm δ_T for all studied metal ions demonstrate the strong interaction between the Fe_3O_4 NPs and the metal ions.

CONCLUSIONS

In this work, ultrafine Fe_3O_4 NPs were successfully synthesized to remove simultaneously four ions (quaternary-metal systems) including Pb^{2+}, Cd^{2+}, Cu^{2+}, and Ni^{2+} from contaminated river water thanks to their mesoporous structure. They were demonstrated as highly effective adsorbents for the removal of multiple metal ions from artificial water and river water. The kinetic models of metal ion adsorption onto Fe_3O_4 NPs fitted perfectly with the pseudo-second-order model both in single and multicomponent systems, illustrating that the processes were chemisorptive in nature. The experimental findings well followed the Langmuir isotherm, indicating that the adsorption mechanism was limited by monolayer coverage. Furthermore, based on the thermodynamic investigations, it was also shown that the adsorption process was spontaneous and endothermic. Eventually, for practical applications, the adsorption/desorption tests demonstrated that the ultrafine Fe_3O_4 NPs were reusable and can be used several times even after five succeeding cycles. The regeneration of Fe_3O_4 NP adsorbents using diluted nitric acid at pH 1.0 indicated that it is quite effective for restoring adsorbents.

EXPERIMENTAL SECTION

Synthesis Procedure of Mesoporous Fe_3O_4 Nanoparticles. The mesoporous hydrophilic Fe_3O_4 nanoparticles were prepared based on the simple and effective coprecipitation of ferric and ferrous salts (Figure S1), as previously reported.[36] Briefly, 250 mL (1.5 M) of NaOH solution and 2 mL of $N_2H_4{\cdot}H_2O$ were added into a three-necked round-bottom flask and heated at 85 °C. Meanwhile, in a clean beaker, 5.2 g of $FeCl_3{\cdot}6H_2O$, 2.0 g of $FeCl_2{\cdot}4H_2O$, and 0.85 mL of HCl (12 M) were dissolved in 25 mL of deionized water at room temperature. The latter mixture was added dropwise to the former one with vigorous stirring. A black precipitate was obtained immediately, which was allowed to crystallize for 30 min under continuous stirring. During the synthesis of the Fe_3O_4 nanoparticles, a nitrogen atmosphere was not used because the decomposition of hydrazine generates N_2 gas.[39] After formation of Fe_3O_4 colloids, the solution was allowed to cool at room temperature. Finally, the black precipitate was filtered off by magnetic decantation, washed with ethanol and deionized water to get rid of the unreacted reactants, and dried in a vacuum oven at 60 °C for 4 h.

Removal Procedure of Heavy Metal Ions in River Water. To test the applicability of Fe_3O_4 nanoadsorbents in natural water, river water was chosen because groundwater and surface water contain a complex mixture of ions. Before being used, river water was filtered by a filter paper to remove all suspended matter. Fe_3O_4 nanoadsorbents (100 mg) were added to 50 mL of river water spiked with 50 mg L^{-1} of each tested ion. The mixture was shaken at 220 rpm at a constant temperature of 25 °C. Then, at regular time intervals, the mixture was withdrawn, the nanoadsorbents were separated by a permanent hand-hold magnet, and the concentration of the remaining ions in the spent solution was determined by an inductively coupled plasma atomic emission spectrophotometer.

ASSOCIATED CONTENT

Supporting Information

The Supporting Information is available free of charge on the ACS Publications website at DOI: 10.1021/acsomega.9b00731.

Experimental section (synthesis of Fe_3O_4, metal ion removal procedure, and point of zero charge); characterization (BET, scanning electron microscope/energy dispersive X-ray analysis); tests of the metal ion adsorption (adsorption kinetics, effect of the temperature, adsorbent dose, initial concentration, and isotherm analysis); thermodynamic studies (PDF)

AUTHOR INFORMATION

Corresponding Author

*E-mail: qiukaipei@ecust.edu.cn. Tel/Fax: 86-21-64252339.

ORCID

Da-Wei Li: 0000-0002-9257-4452

Kaipei Qiu: 0000-0002-9807-9487

Yi-Tao Long: 0000-0003-2571-7457

Notes

The authors declare no competing financial interest.

ACKNOWLEDGMENTS

This work was supported by the National Natural Science Foundation of China (Grant No. 21834001), Innovation Program of Shanghai Municipal Education Commission (Grant No. 2017-01-07-00-02-E00023), and Shanghai Sailing Program (Grant No. 19YF1410400). T.P.F. was supported by the China Scholarship Council for the Ph.D. program in ECUST (CSC No. 2015DFH452).

ABBREVIATIONS

HMI, heavy metal ion; UFMNP, ultrafine magnetite nanoparticle; MNP, magnetic nanoparticle

REFERENCES

(1) Sun, D. T.; Peng, L.; Reeder, W. S.; Moosavi, S. M.; Tiana, D.; Britt, D. K.; Oveisi, E.; Queen, W. L. Rapid, selective heavy metal removal from water by a metal-Organic framework/polydopamine composite. *ACS Cent. Sci.* **2018**, *4*, 349−356.

(2) Lu, X.; Wang, L.; Li, L. Y.; Lei, K.; Huang, L.; Kang, D. Multivariate statistical analysis of heavy metals in street dust of Baoji, NW China. *J. Hazard. Mater.* **2010**, *173*, 744−749.

(3) Rajput, S.; Pittman, C. U.; Mohan, D. Magnetic magnetite (Fe_3O_4) nanoparticle synthesis and applications for lead (Pb^{2+}) and chromium (Cr^{6+}) removal from water. *J. Colloid Interface Sci.* **2016**, *468*, 334−346.

(4) Öztürk, D.; Sahan, T. Design and optimization of Cu (II) adsorption conditions from aqueous solutions by low-cost adsorbent

DOI: 10.1021/acsomega.9b00731
ACS Omega 2019, 4, 7543−7549

pumice with response surface methodology. *Pol. J. Environ. Stud.* **2015**, *24*, 1749−1756.
(5) Fu, F.; Wang, Q. Removal of heavy metal ions from wastewaters: A review. *J. Environ. Manage.* **2011**, *92*, 407−418.
(6) Dave, P. N.; Chopda, L. V. Application of iron oxide nanomaterials for the removal of heavy metals. *J. Nanotechnol.* **2014**, *2014*, 1−14.
(7) Karami, H. Heavy metal removal from water by magnetite nanorods. *Chem. Eng. J.* **2013**, *219*, 209−216.
(8) Amarasinghe, B. M. W. P. K.; Williams, R. A. Tea waste as a low cost adsorbent for the removal of Cu and Pb from wastewater. *Chem. Eng. J.* **2007**, *132*, 299−309.
(9) Kantarli, I. C.; Yanik, J. Activated carbon from leather shaving wastes and its application in removal of toxic materials. *J. Hazard. Mater.* **2010**, *179*, 348−356.
(10) Yantasee, W.; Warner, C. L.; Sangvanich, T.; Addleman, R. S.; Carter, T. G.; Wiacek, R. J.; Fryxell, G. E.; Timchalk, C.; Warner, M. G. Removal of heavy metals from aqueous systems with thiol functionalized superparamagnetic nanoparticles. *Environ. Sci. Technol.* **2007**, *41*, 5114−5119.
(11) Türk, T.; Alp, I. Arsenic removal from aqueous solutions with Fe-hydrotalcite supported magnetite nanoparticle. *J. Ind. Eng. Chem.* **2014**, *20*, 732−738.
(12) Liu, J.; Zhao, Z.; Jiang, G. Coating Fe_3O_4 magnetic nanoparticles with humic acid for high efficient removal of heavy metals in water. *Environ. Sci. Technol.* **2008**, *42*, 6949−6954.
(13) Cutting, R. S.; Coker, V. S.; Telling, N. D.; Kimber, R. L.; Pearce, C. I.; Ellis, B. L.; Lawson, R. S.; Laan, G. V. D.; Pattrick, R. A. D.; Vaughan, D. J.; Arenholz, E.; Lloyd, J. R. Optimizing Cr(VI) and Tc(VII) remediation through nanoscale biomineral engineering. *Environ. Sci. Technol.* **2010**, *44*, 2577−2584.
(14) Wiatrowski, H. A.; Das, S.; Kukkadapu, R.; Ilton, E. S.; Barkay, T.; Yee, N. Reduction of Hg(II) to Hg(0) by magnetite. *Environ. Sci. Technol.* **2009**, *43*, 5307−5313.
(15) Wang, Y.; Morin, G.; Ona-Nguema, G.; Juillot, F.; Calas, G.; Brown, G. E. Distinctive arsenic(V) trapping modes by magnetite nanoparticles induced by different sorption processes. *Environ. Sci. Technol.* **2011**, *45*, 7258−7266.
(16) Kumari, M.; Pittman, C. U.; Mohan, D. Heavy metals [chromium (VI) and lead (II)] removal from water using mesoporous magnetite (Fe_3O_4) nanospheres. *J. Colloid Interface Sci.* **2015**, *442*, 120−132.
(17) Yang, L.; Chen, Z.; Cui, D.; Luo, X.; Liang, B.; Yang, L.; Liu, T.; Wang, A.; Luo, S. Ultrafine palladium nanoparticles supported on 3D self-supported Ni foam for cathodic dechlorination of florfenicol. *Chem. Eng. J.* **2019**, *359*, 894−901.
(18) Giraldo, L.; Erto, A.; Moreno-Piraján, J. C. Magnetite nanoparticles for removal of heavy metals from aqueous solutions: Synthesis and characterization. *Adsorption* **2013**, *19*, 465−474.
(19) Shen, Y. F.; Tang, J.; Nie, Z. H.; Wang, Y. D.; Ren, Y.; Zuo, L. Preparation and application of magnetic Fe_3O_4 nanoparticles for wastewater purification. *Sep. Purif. Technol.* **2009**, *68*, 312−319.
(20) Yuan, P.; Liu, D.; Fan, M.; Yang, D.; Zhu, R.; Ge, F.; Zhu, J.; He, H. Removal of hexavalent chromium [Cr(VI)] from aqueous solutions by the diatomite-supported/unsupported magnetite nanoparticles. *J. Hazard. Mater.* **2010**, *173*, 614−621.
(21) Nassar, N. N. J. Hazard. Mater. Rapid removal and recovery of Pb(II) from wastewater by magnetic nanoadsorbents. *J. Hazard. Mater.* **2010**, *184*, 538−546.
(22) Li, H.; Bian, Z.; Zhu, J.; Zhang, D.; Li, G.; Huo, Y.; Li, H.; Lu, Y. Mesoporous titania spheres with tunable chamber stucture and enhanced photocatalytic activity. *J. Am. Chem. Soc.* **2007**, *129*, 8406−8407.
(23) Hong, R. Y.; Li, J. H.; Li, H. Z.; Ding, J.; Zheng, Y.; Wei, D. G. Synthesis of Fe_3O_4 nanoparticles without inert gas protection used as precursors of magnetic fluids. *J. Magn. Magn. Mater.* **2008**, *320*, 1605−1614.
(24) Faraji, M.; Yamini, Y.; Rezaee, M. Magnetic nanoparticles: synthesis, stabilization, functionalization, characterization, and applications. *J. Iran. Chem. Soc.* **2010**, *7*, 1−37.
(25) Bowen, P. Particle size distribution measurement from millimeters to nanometers and from rods to platelets. *J. Dispersion Sci. Technol.* **2002**, *23*, 631−662.
(26) Faghihian, H.; Nourmoradi, H.; Shokouhi, M. Removal of copper (II) and nickel (II) from aqueous media using silica aerogel modified with amino propyl triethoxysilane as an adsorbent: Equilibrium, kinetic, and isotherms study. *Desalin. Water Treat.* **2014**, *52*, 305−313.
(27) Zein, R.; Suhaili, R.; Earnestly, F.; Munaf, I. E. Removal of Pb(II), Cd(II) and Co(II) from aqueous solution using Garcinia mangostana L. fruit shell. *J. Hazard. Mater.* **2010**, *181*, 52−56.
(28) Criscenti, L. J.; Sverjensky, D. A. The role of electrolyte anions (ClO_4^-, NO_3^-, and Cl^-) in divalent metal (M^{2+}) adsorption on oxide and hydroxide surfaces in salt solutions. *Am. J. Sci.* **1999**, 828−899.
(29) Abuh, M. A.; Akpomie, G. K.; Nwagbara, N. K.; Bassey, N. A.; Ape, D. I.; Ayabie, B. U. Kinetic rate equations application on the removal of copper (II) and zinc (II) by unmodified lignocellulosic fibrous layer of palm tree trunk- single component system studies. *Int. J. Basic Appl. Sci.* **2010**, *1*, 800−809.
(30) Ding, C.; Cheng, W.; Wang, X.; Wu, Z. Y.; Sun, Y.; Chen, C.; Wang, X.; Yu, S. H. Competitive sorption of Pb(II), Cu(II) and Ni(II) on carbonaceous nanofibers: A spectroscopic and modeling approach. *J. Hazard. Mater.* **2016**, *313*, 253−261.
(31) Palin, D., Jr; Rufato, K. B.; Linde, G. A.; Colauto, N. B.; Caetano, J.; Alberton, O.; Jesus, D. A.; Dragunski, D. C. Evaluation of Pb (II) biosorption utilizing sugarcane bagasse colonized by Basidiomycetes. *Environ. Monit. Assess.* **2016**, *188*, 279−293.
(32) Anbia, M.; Kargosha, K.; Khoshbooei, S. Heavy metal ions removal from aqueous media by modified magnetic mesoporous silica MCM-48. *Chem. Eng. Res. Des.* **2015**, *93*, 779−788.
(33) Liu, X.; Hu, Q.; Fang, Z.; Zhang, X.; Zhang, B. Magnetic chitosan nanocomposites: A useful recyclable tool for heavy metal ion removal. *Langmuir* **2009**, *25*, 3−8.
(34) Gong, J.; Wang, X.; Shao, X.; Yuan, S.; Yang, C.; Hu, X. Adsorption of heavy metalions by hierarchically structured magnetite-carbonaceous spheres. *Talanta* **2012**, *101*, 45−52.
(35) Uluozlu, O. D.; Tuzen, M.; Mendil, D.; Soylak, M. Coprecipitation of trace elements with $Ni^{2+}/^{2-}$ nitroso-1-naphthol-4-sulfonic acid and their determination by flame atomic absorption spectrometry. *J. Hazard. Mater.* **2010**, *176*, 1032−1037.
(36) Li, J.; Zhao, X.; Shi, Y.; Cai, Y.; Mou, S.; Jiang, G. Mixed hemimicelles solid-phase extraction based on cetyltrimethylammonium bromide-coated nano-magnets Fe_3O_4 for the determination of chlorophenols in environmental water samples coupled with liquid chromatography / spectrophotometry detection. *J. Chromatogr. A* **2008**, *1180*, 24−31.
(37) Shahryari, Z.; Goharrizi, A. S.; Azadi, M. Experimental study of methylene blue adsorption from aqueous solutions onto carbon nano tubes. *Int. J. Water Resour. Environ. Eng.* **2010**, *2*, 16−28.
(38) Fan, T.; Liu, Y.; Feng, B.; Zeng, G.; Yang, C.; Zhou, M.; Zhou, H.; Tan, Z.; Wang, X. Biosorption of cadmium(II), zinc(II) and lead(II) by penicillium simplicissimum: Isotherms, kinetics and thermodynamics. *J. Hazard. Mater.* **2008**, *160*, 655−661.
(39) Singh, M.; Kumar, M.; Štěpánek, F.; Ulbrich, P.; Svoboda, P.; Santava, E.; Singla, M. L. Liquid-phase synthesis of nickel nanoparticles stabilized by PVP and study of their structural and magnetic properties. *Adv. Mater. Lett.* **2011**, *2*, 409−414.

DOI: 10.1021/acsomega.9b00731
ACS Omega 2019, 4, 7543−7549